

Coupling of MEMS ultrasonic transducers

D.W. Greve

Dept. Electrical and Computer Engineering
Carnegie Mellon University
Pittsburgh, PA, USA
dg07@andrew.cmu.edu

I.J. Oppenheim

Department of Civil and Environmental Engineering
Carnegie Mellon University
Pittsburgh, PA, USA
ijjo@andrew.cmu.edu

Abstract

MEMS ultrasonic transducers are potentially valuable in both medical and non-destructive testing applications. A prime advantage of these transducers is their wide bandwidth together with the potential for economical fabrication of detector arrays. In this paper, we discuss issues related to the coupling of these transducers to solid and liquid media. We will show that appropriate choice of the coupling medium thickness is required in order to prevent spurious pulses.

Keywords

MEMS, ultrasonic, capacitive, transducer

INTRODUCTION

MEMS ultrasonic transducers (sometimes termed cMUTs, for capacitive MEMS Ultrasonic Transducers), have been studied by several research groups [1,2,3,4,5,6] both for liquid immersion applications [1,2,3,4] and also in contact with solid media [5,6]. In general, ultrasonic transducers are used to generate short pulses which propagate in a solid or liquid medium. Flaws or discontinuities in the medium cause reflected pulses which are then detected and displayed. In general, a wide bandwidth around the pulse center frequency is desirable in order to distinguish closely spaced reflections. MEMS capacitive transducers offer very high bandwidth compared to conventional piezoelectric transducers as a consequence of the small acoustic impedance relative to the solid and liquid media of interest [ours, theirs]. However, there remain important issues of transducer fragility, efficiency of generation of ultrasonic energy, and coupling of the transducer to the transmitting medium.

In this paper we focus on the issue of acoustic coupling. We will illustrate coupling of MEMS transducers to both solid and liquid media. Experiments and simulations show that careful control of the thickness of the coupling medium will be required for good performance. Experimental results will concern the receive performance only. The transducers we discuss are not efficient transmitters, and are best used in conjunction with piezoelectric transmitters. The development of efficient transmitters has been a focus of other work [7,8].

ACOUSTIC EQUIVALENT CIRCUIT

Figure 1 shows a cross section of one unit of a capacitive ultrasonic transducer. Our ultrasonic transducers have been fabricated using the multi-user MUMPS process using the POLY0 and POLY1 electrodes. The POLY1 thickness is 2 μm and the gap between the POLY0 and POLY1 electrodes is 2.0 μm. The sacrificial insulator between the electrodes is removed by etching through 5 μm square etch holes. The transducer used in this work has 180 identical units each with bottom plate consisting of a hexagon with 45 μm edge length.

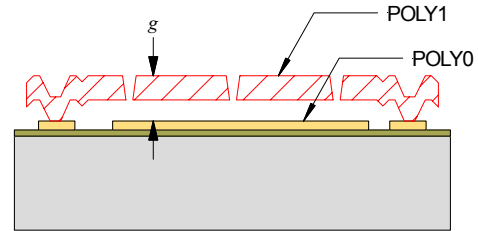


Figure 1. One unit of a capacitive diaphragm transducer.

When an incident ultrasonic wave strikes the transducer, the upper plate vibrates with a velocity $u(t)$ with respect to the lower plate. If a DC bias V_{DC} is applied between the two plates, the transducer current $i(t)$ will be given by

$$i(t) = V_{DC} \frac{\epsilon_0 S}{g^2} \frac{dx}{dt} = V_{DC} \frac{\epsilon_0 S}{g^2} u(t)$$

where ϵ_0 is the permittivity of free space, S is the surface area of the transducer, and g is the gap between the two electrodes.

The acoustic coupling between the transmitting medium and the transducer can be modeled by the equivalent circuit shown in Fig. 2. The transmission lines representing the transmitting medium and the coupling medium have acoustic impedances Z_m and Z_c respectively.

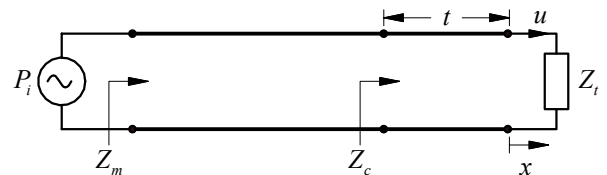


Figure 2. Equivalent circuit for coupling between a solid medium with acoustic impedance Z_m and a detector with acoustic impedance Z_t .

The acoustic impedance of the transducer Z_t can be predicted based on the diaphragm dimensions or alternatively can be extracted from electrical measurements [9]. Figure 3 plots the extracted acoustic impedance for the transducer used here.

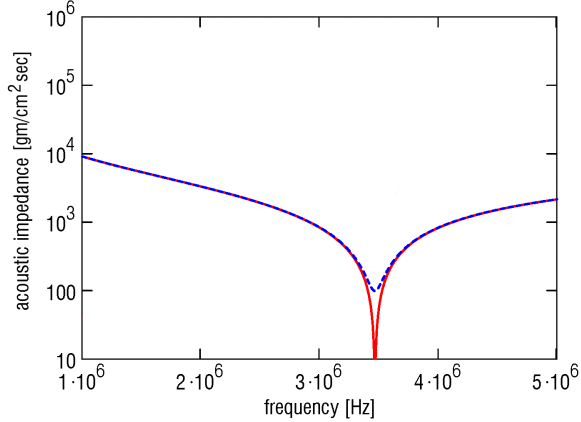


Figure 3. Acoustic impedance of capacitive diaphragm transducer: (dashed line) diaphragm loaded by air and (solid line) diaphragm in vacuum.

Table I shows the acoustic impedances of several relevant transmitting materials [10]. It is important to note that, with the exception of air, all of these materials have acoustic impedances considerably larger than the diaphragm acoustic impedance. Thus, to a good approximation, we can treat the diaphragm as an acoustic short circuit ($Z_t=0$).

Table I. Acoustic properties of various materials.

material	Z_m [gm/cm ² sec]	v_{long} [cm/sec]
air	0.0004×10^5	0.33×10^5
water	1.48×10^5	1.48×10^5
plexiglas	3.1×10^5	2.7×10^5
aluminum	17×10^5	6.3×10^5
steel	46×10^5	3.2×10^5

In the following, we will explore the effect of various coupling arrangements. The transmission line equivalent circuit of Fig. 2 will be used where the transmission lines will be considered lossless.

We first consider the case in which the coupling medium is equal in acoustic impedance to the transmitting medium (or alternatively the case in which the transducer is bonded directly to the transmitting medium). In this case the transducer imposes the boundary condition

$$\frac{P(0)}{u(0)} = Z_t \approx 0$$

where P is the acoustic pressure and u is the particle velocity. The acoustic waves consist of waves moving in the $+x$ and $-x$ directions given by [11]

$$P(x,t) = P^+ e^{j(\omega t - kx)} + P^- e^{j(\omega t + kx)}$$

$$u(x,t) = \frac{P^+}{Z_t} e^{j(\omega t - kx)} - \frac{P^-}{Z_t} e^{j(\omega t + kx)}$$

Imposing the boundary condition at $x = 0$ yields $P^+ \approx -P^-$ so we conclude that

$$u(0,t) = \frac{2P^+}{Z_t} e^{j\omega t}$$

where P^+ is the amplitude of the incident wave.

Note that in this case there is a large reflected wave, equal in magnitude to the incident wave. Reflected waves cause problems if there are impedance discontinuities which can give rise to additional reflections. In order to understand the issues which arise, we need to consider the transmission of pulses rather than sinusoids.

In order to examine the propagation of pulses, we have used the circuit analysis program PSPICE. Figure 4 shows the circuit used for simulation. The series RLC combination is the acoustic impedance of the transducer as extracted from electrical measurements [12]. In these simulations, an impedance of 1Ω (electrical) corresponds to $1 \text{ gm/cm}^2\text{sec}$ (acoustic). Pressure is analogous to voltage and velocity corresponds to electric current.

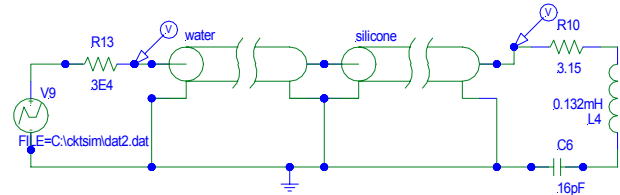


Fig. 4. Circuit for simulation of acoustic propagation using SPICE.

Simulations were performed using as an input a short pulse (width approximately $0.6 \mu\text{s}$) with a center frequency of 5 MHz. The waveform of the incident pulse is shown in Fig. 5. This is a reasonable approximation to the pulse shapes produced by commercial PZT transducers.

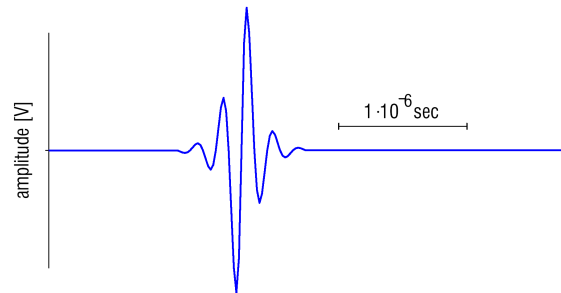


Figure 5. Incident pulse shape.

ACOUSTIC COUPLING ($t \ll \lambda/4$)

We first consider the case of very thin coupling layers. For simulation purposes, we have assumed an acoustic impedance for the coupling layer of $2 \times 10^5 \text{ gm/cm}^2\text{sec}$ [13] and a thickness of 0.025 mm. Coupling layers of this thickness

were used in our experiments on MEMS transducer coupling to plexiglas [5].

Figure 6 shows the calculated pressure and diaphragm velocity for this case. In this figure both pressure and diaphragm velocity accurately reproduce the shape of the incident pulse.

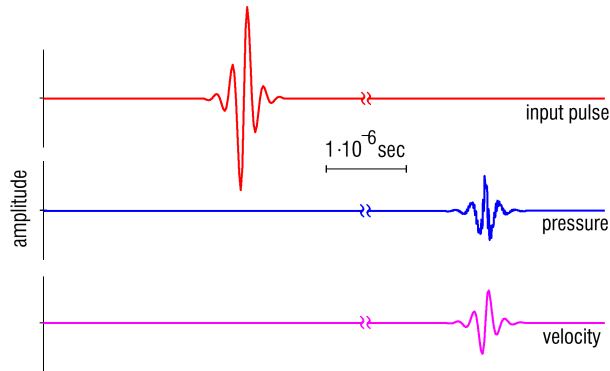


Figure 6. Simulations with thin ($t = 0.025$ mm) coupling layer: (top) input pulse, (middle) pressure at capacitive diaphragm transducer and (bottom) velocity at capacitive diaphragm transducer.

These predictions are consistent with the results of pulse propagation experiments. In these experiments a commercial PZT transducer (Krautkramer MSW-QC) driven by a Krautkramer USPC-2100 pulser/ display unit was used to create short ultrasonic pulses. For example, Fig. 7 shows received signals for excitation at 3.5 MHz; at this center frequency the coupling layer is an even smaller fraction of a wavelength. Figure 7 (top) shows the experimental specimen which contains two holes simulating voids in a structural specimen. The received pulses are narrow and the individual reflections are clearly discernable.

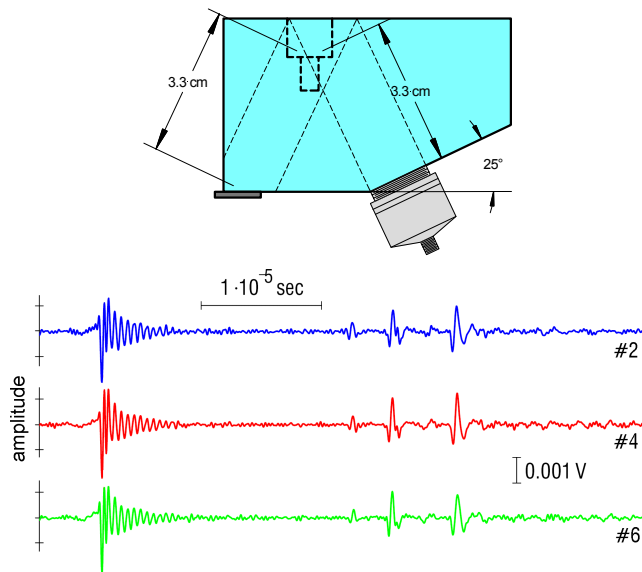


Figure 7. Received ultrasonic signals for MEMS transducer chip coupled by thin ($t = 0.025$ mm) silicone: (top) geometry of test specimen and (bottom) received transients from three capacitive transducers.

ACOUSTIC COUPLING ($t > \lambda/4$)

Thicker coupling layers are desirable in the case of transducers which are liquid-coupled. In this case the coupling layer serves several purposes. In addition to providing for transmission of ultrasonic energy, the coupling layer also provides electrical insulation between the electrodes and the transmitting medium and in addition a degree of mechanical protection. Thick layers are obviously preferred for electrical insulation and mechanical protection. We will show however that increasing the thickness degrades the ultrasonic pulsewidth, and in extreme cases can result in spurious reflections.

Figure 8 shows an ultrasonic transducer chip which has been attached to a 40-pin ceramic package with epoxy and wirebonded to the package terminals. The cavity has been filled with silicone (Gelest Zipcone CG) so that the package and the bond wires are encapsulated.

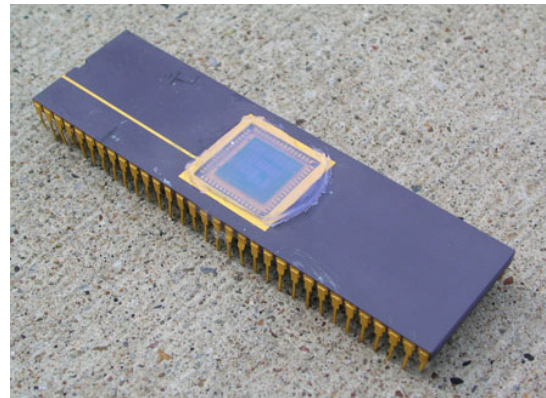


Figure 8. Photograph of ultrasonic transducer chip attached to ceramic package and coated with silicone.

Possible failure mechanisms during packaging include damage of the fragile transducer membranes, penetration of silicone into the etch release holes, and detachment of the bond wires. We have found that transducers are sufficiently durable for the silicone coating process. Ultrasonic transducers encapsulated in this way are unaffected by extended exposure in water (~ 2 days) and are mechanically robust [14]. In some experiments the silicone thickness was as large as 0.15 cm. The silicone layer thickness depends on the amount of silicone applied and can be reduced to at least 0.03 cm.

Figure 9 shows the predicted pulse response for various silicone thicknesses. The transmitting medium in these simulations is water and the silicone acoustic impedance is assumed to be 2×10^5 gm/cm²sec. The measured velocity in silicone is approximately 1.5×10^5 cm/sec so the traces in Fig. 9 correspond to thicknesses of 0.0075, 0.015, and 0.03 cm.

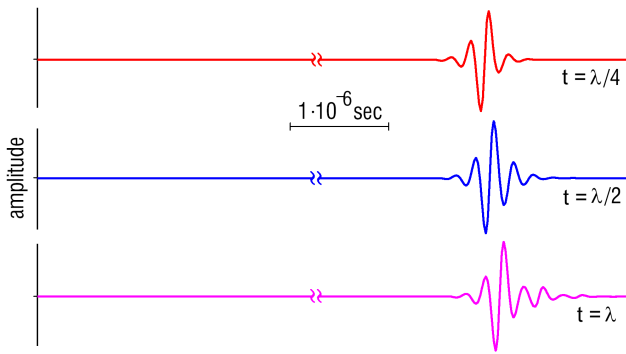


Figure 9. Simulated velocity at receiver for three different coupling layer thicknesses: $t = \lambda/4$ (0.0075 cm), $t = \lambda/2$ (0.015 cm), and $t = \lambda$ (0.03 cm).

The simulations show that the pulse shape is visibly degraded for silicone layer thicknesses of $\lambda/2$ and greater. Physically the degraded pulse shape is a consequence of reflections within the silicone layer. These reflections are negligible if the acoustic impedance of the transmitting medium is equal to that of the coupling medium.

When the coupling medium is thick reflections within the coupling layer may give rise to spurious pulses. This is shown in Fig. 10 where the path length in water is $9 \mu\text{s}$ and coupling layer is assumed to be 0.15 cm in thickness. This figure shows the pressure at the diaphragm together with the pressure at the emitting transducer. Thus the figure shows not only the signal measured by the capacitive diaphragm transducer but also the signal which would be observed at the PZT transducer in receive mode.

Consider first the blue (lower) trace in Fig. 10. The first pulse received is at about $10.2 \mu\text{s}$ after the exciting pulse which corresponds to the path length in water plus the time to traverse the silicone coupling layer

$$\tau = t / c_{\text{silicone}} = 1.2 \mu\text{s}.$$

A second smaller pulse appears at the diaphragm approximately $2.4 \mu\text{s}$ later. This pulse is a reflection from the diaphragm which reflects again at the silicone-water interface and then returns to the diaphragm. A third, much smaller pulse is also barely visible another $2.4 \mu\text{s}$ later.

The upper (red) trace shows the signal which would be detected at the PZT transducer position. The first small pulse approximately $18 \mu\text{s}$ after the exciting pulse corresponds to reflection at the silicone-water interface, while the second larger pulse is due to reflection from the diaphragm (adding one round-trip time in the silicone layer). The third pulse corresponds to two reflections off the diaphragm and two round-trip delays in the silicone. Note that with ideal lossless transmission lines additional pulses result from reflections at the emitting transducer.

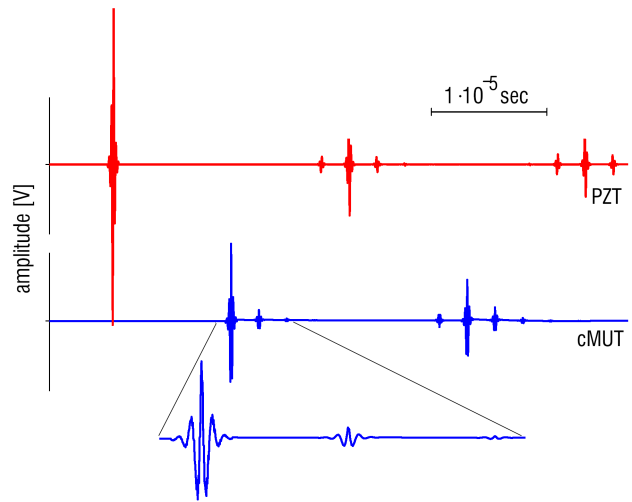


Figure 10. Simulated signals observed at (top) PZT emitter and (bottom) cMUT receiver. The silicone thickness was 0.15 cm and the silicone acoustic impedance was $2.0 \times 10^5 \text{ gm/cm}^2\text{-sec}$.

We will now compare these simulations with experimental observations on transducers with thick coupling layers. Figure 11 shows the experimental configuration, where a commercial PZT transducer is used as the transmitter and a capacitive transducer as a receiver. The transmitting medium is water with variable path length.

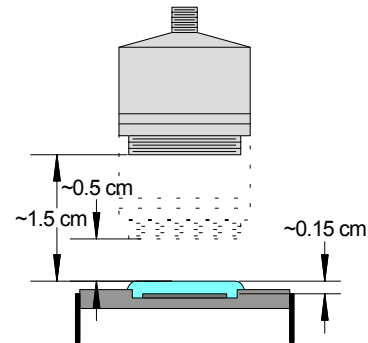


Fig. 11. Arrangement for measurements with water coupling.

Figure 12 shows the experimental results for two path lengths in water. The emitted pulse is at $t = 5 \mu\text{s}$ and produces a small transient in the PZT trace and the capacitive transducer trace (this transient is due to stray electrical coupling). The signal received by the capacitive transducer shows two pulses separated by approximately $2.4 \mu\text{s}$, which agrees well with the expected path length in silicone. At the PZT transducer, we see a single broad transient rather than three sharp pulses as in the simulation (Fig. 10). This indicates that the one-dimensional transmission line model is overly idealized. Possibly the pulse is spread out due to reflections from both the transducer area and the ceramic package. The lower pair of traces shows that all pulses move as expected when the path length in water is reduced.

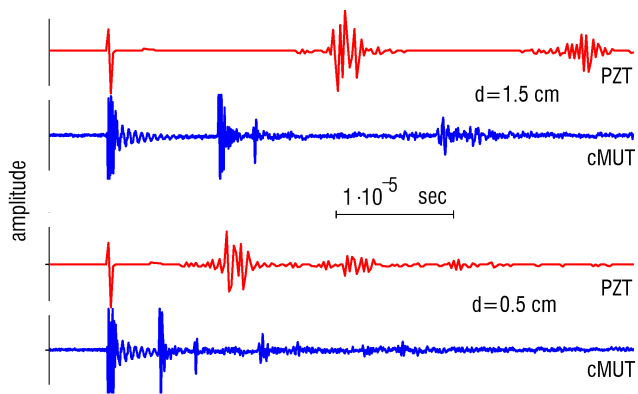


Figure 12. Liquid coupling with thick (~0.15 cm) silicone layer: (top) 1.5 cm water path length and (bottom) 0.5 cm water path length. The red traces show the reflected pulses received by the PZT transducer and the blue traces show the signal observed by the capacitive transducer.

We previously measured and reported an acoustic impedance for Gelest CG silicone of $1.5 \times 10^5 \text{ gm/cm}^2\text{-sec}$ [5], which is almost exactly that of water. In theory we would expect *no* reflections at the water-silicone interface, but our experiments showed such reflections to be present. We performed the simulations shown in Fig. 11 using an assumed silicone acoustic impedance of $2.0 \times 10^5 \text{ gm/cm}^2\text{-sec}$, which yielded reflected pulses of approximately the correct magnitude, and we note that plastics and rubbers have acoustic impedances in the range $2\text{-}3 \times 10^5 \text{ gm/cm}^2\text{-sec}$ [10]. These observations suggest that our assumed acoustic impedance of 2.0×10^5 is reasonable and that our measured acoustic impedance of 1.5×10^5 is substantially too low. However, the measurement errors in our earlier determination of the silicone acoustic impedance are not large enough to account for this difference; it is possible that the acoustic impedance of thin layers of silicone, as used in our experiments, is higher than the acoustic impedance in bulk specimens, as used in our measurement of acoustic impedance, because of drying effects.

SUMMARY AND CONCLUSIONS

MEMS capacitive transducers can be used to detect ultrasonic pulses in both liquid and solid transmitting media. However, acoustic coupling of these transducers to the transmitting medium is an important issue. The acoustic properties of the coupling medium and its thickness can have a major effect on the received pulse shape and can even introduce spurious pulses.

We have shown that most features of the received pulse shape can be understood using a one-dimensional transmission line model. Coupling layers substantially less than an acoustic wavelength in thickness have essentially no impact on the pulse shape. As the thickness of the coupling layer is increased, the received pulse is first slightly broadened and distorted and separates into multiple pulses for very thick

coupling layers. Pulse distortion and spurious pulses will be a particularly serious problem when the transmitting and coupling media are very different in acoustic impedance.

ACKNOWLEDGEMENTS

This work is supported by the National Science Foundation under grant CMS-0329880 and by the Commonwealth of Pennsylvania through the Pennsylvania Infrastructure Technology Alliance program. The authors would also like to acknowledge gifts from Krautkramer Inc.

REFERENCES

- [1] "Surface micromachined ultrasound transducers in CMOS technology," P.-C. Eccardt, K. Niederer, T. Scheiter, and C. Hierold, 1996 IEEE Ultrasonics Symposium, pp. 959-962 (1996).
- [2] "Micromachined ultrasonic capacitance transducers for immersion applications," A.G. Bashford, D.W. Schindel, D.A. Hutchins, IEEE Transactions on Ultrasonics, Ferroelectrics, and Frequency Control, vol. 45, pp. 367-375 (1998).
- [3] "Characterization of one-dimensional capacitive micromachined ultrasonic immersion transducer arrays," X. Jin, I. Ladabaum, F.L. Degertekin, S. Calmes, and B.T. Khuri-Yakub, IEEE Journal of Microelectromechanical Systems, vol. 8, pp. 100-114 (1999).
- [4] X. Jin, O. Oralkan, F.L. Degertekin, and B.T. Khuri-Yakub, "Characterization of one-dimensional capacitive micromachined ultrasonic immersion transducer arrays," IEEE Transactions on Ultrasonics, Ferroelectrics, and Frequency Control, vol. 48, pp. 750-760 (2001).
- [5] "MEMS Ultrasonic Transducers for the Testing of Solids," I.J. Oppenheim, A. Jain, and D.W. Greve, IEEE Transactions on Ultrasonics, Ferroelectrics, and Frequency Control, vol. 50, pp. 305-311 (2003).
- [6] "MEMS Phased Array Detection in Contact with Solids," D.W. Greve, A. Jain, and I.J. Oppenheim, 2002 IEEE Ultrasonics Symposium, paper 5D-6.
- [7] "Broadband capacitive micromachined ultrasonic transducers ranging from 10 kHz to 60 MHz for imaging arrays and more," A.S. Ergun, Y. Huang, C.-H. Cheng, O. Oralkan, J. Johnson, H. Jagannathan, U. Demirci, G.G. Yaraliglu, M. Karaman, and B.T. Khuri-Yakub, 2002 IEEE Ultrasonics Symposium p. 1039.
- [8] "Theory of a Double-Diaphragm MEMS Ultrasonic Transducer," D.W. Greve and I.J. Oppenheim, (to be published in Proc. IEEE UFFC 2003).
- [9] "Electrical Characterization of Coupled and Uncoupled MEMS Ultrasonic Transducers," I.J. Oppenheim, A. Jain, and D.W. Greve, IEEE Transactions on Ultrasonics, Ferroelectrics, and Frequency Control, vol. 50, pp. 297-304 (2003).
- [10] "Ultrasonic Transducers For Nondestructive Testing," catalog published by Krautkramer, Inc., (April 2001).

- [11] See, for example, *Electromagnetic Concepts and Applications*, G.G. Skitek and S.V. Marshall, p. 372 (Prentice-Hall, Englewood Cliffs, NJ, 1978)
- [12] "Electrical Characterization of Coupled and Uncoupled MEMS Ultrasonic Transducers," I.J. Oppenheim, A. Jain, and D.W. Greve, *IEEE Transactions on Ultrasonics, Ferroelectrics, and Frequency Control*, vol. 50, pp. 297-304 (2003).
- [13] This value disagrees with a previous measurement of ours as will be discussed later in this paper.
- [14] "Robust Capacitive MEMS Ultrasonics Transducers for Liquid Immersion," D.W. Greve, J. Neumann, I.J. Oppenheim, D. Ozevin, and S.P. Pessiki, (to be published in *Proc. IEEE UFFC 2003*).
- [15] "Ultrasonic Transducers For Nondestructive Testing," catalog published by Krautkramer, Inc., (April 2001).

**DO NOT DELETE THIS PAGE ALL REFERENCES
WILL DISAPPEAR**

¹ "Surface micromachined ultrasound transducers in CMOS technology," P.-C. Eccardt, K. Niederer, T. Scheiter, and C. Hierold, 1996 IEEE Ultrasonics Symposium, pp. 959-962 (1996).

² "Micromachined ultrasonic capacitance transducers for immersion applications," A.G. Bashford, D.W. Schindel, D.A. Hutchins, IEEE Transactions on Ultrasonics, Ferroelectrics, and Frequency Control, vol. 45, pp. 367-375 (1998).

³ "Characterization of one-dimensional capacitive micromachined ultrasonic immersion transducer arrays," X. Jin, I. Ladabaum, F.L. Degertekin, S. Calmes, and B.T. Khuri-Yakub, IEEE Journal of Microelectromechanical Systems, vol. 8, pp. 100-114 (1999).

⁴ X. Jin, O. Oralkan, F.L. Degertekin, and B.T. Khuri-Yakub, "Characterization of one-dimensional capacitive micromachined ultrasonic immersion transducer arrays," *IEEE Transactions on Ultrasonics, Ferroelectrics, and Frequency Control*, vol. 48, pp. 750-760 (2001).

⁵ "MEMS Ultrasonic Transducers for the Testing of Solids," I.J. Oppenheim, A. Jain, and D.W. Greve, IEEE Transactions on Ultrasonics, Ferroelectrics, and Frequency Control, vol. 50, pp. 305-311 (2003).

⁶ "MEMS Phased Array Detection in Contact with Solids," D.W. Greve, A. Jain, and I.J. Oppenheim, 2002 IEEE Ultrasonics Symposium, paper 5D-6.

⁷ "Broadband capacitive micromachined ultrasonic transducers ranging from 10 kHz to 60 MHz for imaging arrays and more," A.S. Ergun, Y. Huang, C.-H. Cheng, O. Oralkan, J. Johnson, H. Jagannathan, U. Demirci, G.G. Yaraliglu, M. Karaman, and B.T. Khuri-Yakub, 2002 IEEE Ultrasonics Symposium p. 1039.

⁸ "Theory of a Double-Diaphragm MEMS Ultrasonic Transducer," D.W. Greve and I.J. Oppenheim, (to be published in Proc. IEEE UFFC 2003).

⁹ "Electrical Characterization of Coupled and Uncoupled MEMS Ultrasonic Transducers," I.J. Oppenheim, A. Jain, and D.W. Greve, IEEE Transactions on Ultrasonics, Ferroelectrics, and Frequency Control, vol. 50, pp. 297-304 (2003).

¹⁰ "Ultrasonic Transducers For Nondestructive Testing," catalog published by Krautkramer, Inc., (April 2001).

¹¹ See, for example, Electromagnetic Concepts and Applications, G.G. Skitek and S.V. Marshall, p. 372 (Prentice-Hall, Englewood Cliffs, NJ, 1978)

¹² "Electrical Characterization of Coupled and Uncoupled MEMS Ultrasonic Transducers," I.J. Oppenheim, A. Jain, and D.W. Greve, IEEE Transactions on Ultrasonics, Ferroelectrics, and Frequency Control, vol. 50, pp. 297-304 (2003).

¹³ This value disagrees with a previous measurement of ours as will be discussed later in this paper.

¹⁴ "Robust Capacitive MEMS Ultrasonics Transducers for Liquid Immersion," D.W. Greve, J. Neumann, I.J. Oppenheim, D. Ozevin, and S.P. Pessiki, (to be published in Proc. IEEE UFFC 2003).